

Bessel's improved Kater pendulum in the teaching lab

D. Candela,^{a)} K. M. Martini,^{b)} R. V. Krotkov, and K. H. Langley
Physics Department, University of Massachusetts, Amherst, Massachusetts 01003

(Received 9 November 2000; accepted 19 December 2000)

We describe a Bessel pendulum for use in the teaching laboratory, and measurements of the local acceleration of gravity made with it to an accuracy of better than one part in 10^4 . The Bessel pendulum is a reversible pendulum that eliminates atmospheric corrections that apply to the more familiar Kater pendulum. The physical principles underlying the Kater pendulum as well as Bessel's refinement are reviewed, and construction details are given for a realization of the pendulum.

© 2001 American Association of Physics Teachers.

[DOI: 10.1119/1.1349544]

I. INTRODUCTION

Most undergraduate physics students learn about the physical pendulum (a rigid body pivoted about an arbitrary axis), and a few undergraduate mechanics texts treat the Kater pendulum.^{1,2} This is a physical pendulum built so that it can be pivoted about two different parallel axes on the body. When the pendulum is adjusted so that the frequencies of small oscillations about the two pivots are equal, the relationship between the angular frequency ω_0 and the distance Δx between the pivots is

$$\omega_0^2 = g/\Delta x. \quad (1)$$

This superficially resembles the equation for the frequency of a simple pendulum (point mass and string), and enables determination of the acceleration of gravity g without knowing the moment of inertia or center-of-mass location of the pendulum. As discussed below, Eq. (1) is generally only true when the center of mass of the pendulum is between the two pivots and closer to one of them. The principle expressed by this equation was discussed by Huygens as early as 1673. Based on this principle, de Prony proposed an invertible pendulum for the measurement of g in 1800, and a similar proposal was published by Bohnenberger in 1811. However, de Prony's and Bohnenberger's ideas were not accepted at the time and it was left to Henry Kater to design, implement, and popularize the invertible pendulum for gravity measurements, starting in 1817.³

A clever improvement to the Kater pendulum devised by Bessel in 1826⁴ is apparently much less familiar to present-day physicists. The frequency of a Kater pendulum deviates from Eq. (1) due to several effects that result from the surrounding atmosphere, namely the buoyancy of the pendulum and mass of air that is dragged along with the pendulum. Bessel showed that these two effects of the atmosphere vanish if the pendulum is made with a symmetric *shape*, despite its necessarily asymmetric *mass distribution*. Bessel also showed how effects of rounding of the knife-edge pivots could be made to cancel out, as discussed briefly in Appendix B below.

We will call a symmetrically shaped reversible pendulum a Bessel pendulum.⁵ One hundred years ago, carefully constructed Bessel pendulums were the most accurate instruments available for absolute measurements of the acceleration of gravity.⁶ Since that time, several advances have made this technology obsolete. The availability of good vacuum pumps has obviated the need to correct for atmospheric effects, and more recently laser-interferometric measurement

of the trajectory of a freely falling object has supplanted the pendulum altogether in absolute measurements of g .⁷

Inspired by the pedagogical virtues reported for earlier simple-pendulum,⁸ Kater-pendulum,⁹ and conical-pendulum¹⁰ experiments, we have constructed a Bessel pendulum for use in the teaching laboratory. The principles behind its operation include instructive lessons in mechanics and fluid mechanics, and it is not much more difficult to construct than an ordinary Kater pendulum. The plan of this paper is as follows. Sections II and III treat the basic physics behind the Kater pendulum and Bessel's improvement to it, respectively. Section IV describes the Bessel pendulum that we have constructed and operated.

II. THE KATER PENDULUM WITHOUT AIR CORRECTIONS

The following derivation for the operation of the Kater pendulum makes it clear why the center of mass generally is not midway between the two pivot points. We start with the expression for the angular frequency ω for small oscillations of a physical pendulum,

$$\omega^2 = gml/I, \quad (2)$$

where m is the mass of the pendulum, l is the distance between the pivot axis and the center of mass, and I is the moment of inertia about the pivot.^{1,2} Consider a physical pendulum that can be pivoted about any of a series of axes that intersect a chosen line through the center of mass. The pivot axes are all parallel to one another, and perpendicular to the line. Let x denote the position of the pivot axis along the line, relative to an arbitrary origin on the pendulum. Let the center of mass be at $x = x_c$, where we take $x_c \geq 0$ without loss of generality. For convenience we define the function $F(x) = \omega^2/g$. By Eq. (2) this function satisfies

$$F(x) = \frac{m|x - x_c|}{I} = \frac{m|x - x_c|}{I_0 + m(x - x_c)^2}. \quad (3)$$

Here the parallel-axis theorem has been used to express the moment of inertia I about the pivot point in terms of the moment of inertia I_0 about the center of mass. The absolute value in Eq. (3) is needed for a reversible pendulum, as the pivot point x can be on either side of the center-of-mass location x_c .

The shape of the curve $F(x)$ can be deduced by inspection of Eq. (3): It is symmetric about the point $x = x_c$, and goes to zero both at $x = x_c$ and for $x \rightarrow \pm\infty$ (Fig. 1). To find graphi-

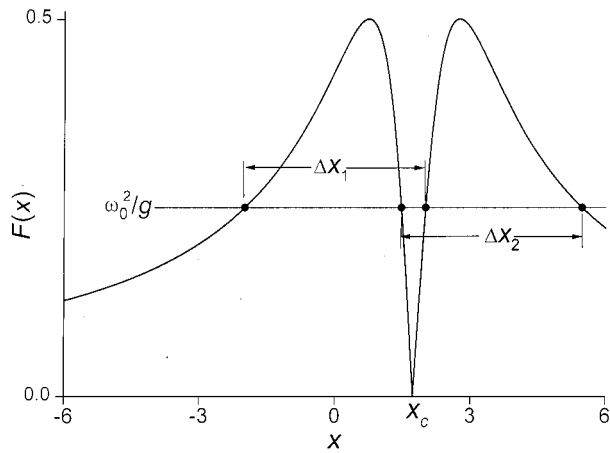


Fig. 1. The function $F(x) = \omega^2/g$ relating the frequency ω of a physical pendulum without air corrections to the pivot axis location x . The frequency vanishes when the pendulum is pivoted at the center-of-mass location x_c . In general there are four pivot axis locations x for which the pendulum oscillates at a given frequency ω_0 , shown by the intersections with the horizontal line $F = \omega_0^2/g$. Of the six possible interpivot distances, only Δx_1 and Δx_2 satisfy the Kater condition, and only Δx_1 is possible for a Bessel pendulum with pivots symmetric about $x=0$. For this schematic plot we have suppressed units and chosen $m = I_0 = 1$, $x_c = \sqrt{3}$, $\omega_0^2/g = 1/4$.

cally the set of pivot points x about which the pendulum oscillates at a given frequency ω_0 , we find the intersection of the curve $F(x)$ with the horizontal line $F_0 \equiv \omega_0^2/g$. In general there are *four* such points (or none), so there are four different pivot points along the pendulum with the same oscillation frequency. Due to the symmetry of $F(x)$, the four pivots for a specified oscillation frequency are symmetrically located about the center of mass, even if the pendulum itself has no symmetry (Fig. 2). Obviously the Kater relation, Eq. (1), between frequency and distance between pivot points can only be true for some of the six possible distances between these four points!

To find which pivot points satisfy the Kater relation, define $y = x - x_c$ and set $F(y) = m|y|/(I_0 + my^2) = F_0$. This yields a quadratic equation in y with roots

$$y = \pm \frac{1}{2F_0} \pm \sqrt{\frac{1}{4F_0^2} - \frac{I_0}{m}}. \quad (4)$$

The two indeterminate signs in this equation may be chosen independently, giving the four possible pivot points for frequency ω_0 . The first sign determines which side of the center of mass the pivots are on, while the second sign further distinguishes between the locations of the pivots on that side. If we pick the pivot closer to the center of mass on one side and the pivot further away from the center of mass on the other side, then the radical in Eq. (4) cancels when the distance between pivots is calculated, giving

$$\Delta x = \Delta y = 1/F_0 = g/\omega_0^2. \quad (5)$$

This is the Kater condition, Eq. (1). Conversely, if we pick two points from Eq. (4) symmetric about the center of mass or two points on the same side of the center of mass, the radical does not cancel. For these choices we are left with a complicated expression for Δx that involves the moment of

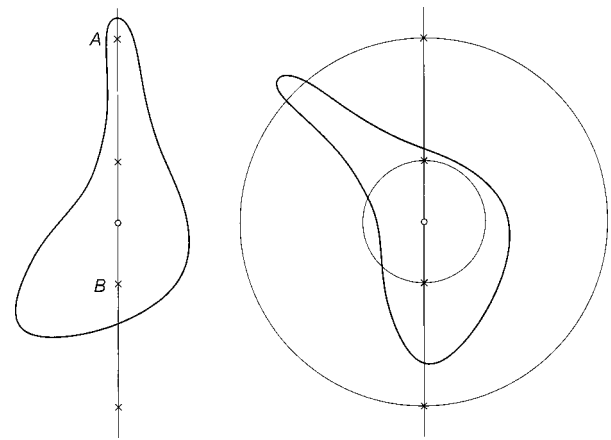


Fig. 2. (Left) Sketch of an arbitrarily shaped body with an arbitrarily chosen line passing through the center of mass (circle). The crosses show four pivot axes that have the same oscillation frequency, determined as in Fig. 1. The four axes are symmetrically located about the center of mass, even if the body has no symmetry. Here one of four pivot axes lies outside the body (one should imagine a rigid, massless support connecting the pivot to the body). Pivots A and B are suitable for use of the body as a Kater pendulum without air corrections. (Right) Here the body has been rotated to emphasize that *any* line of pivots through the center of mass can be used. The oscillation frequency about the crosses is the same as for the left-hand side, assuming all pivot axes are perpendicular to the page. The oscillation frequency is the same for pivots anywhere on the two circles shown centered on the center of mass.

inertia I_0 . Thus only two of the six possible interpivot distances satisfy the Kater condition, and the center of mass is generally *not* centered between the pivots for either of these two choices (Δx_1 and Δx_2 in Fig. 1).

III. AIR CORRECTIONS AND BESSEL'S REVERSIBLE PENDULUM

As shown above, the mass distribution of a Kater pendulum is necessarily asymmetric with respect to the pivot points. Bessel showed that if the *volume* distribution of the pendulum is nevertheless made symmetric about the point midway between the pivots, two important air corrections disappear allowing the simple Kater condition to be applied. These are the corrections for buoyancy of the pendulum in air and for the inertia due to air dragged by the pendulum as it oscillates.¹¹

For the following discussion, assume the volume distribution (i.e., the shape) of the pendulum to be symmetric about the point $x=0$. The center of mass is at $x = x_c > 0$, as above. The effect of buoyancy is to reduce the effective weight of the pendulum by the weight of the air it displaces, $m_b g$. That is to say, the *gravitational* mass of the pendulum is effectively reduced by m_b , while the *inertial* mass is unaffected. This leads to a decrease in the numerator of Eq. (3), which is proportional to the gravitational torque on the pendulum:

$$m|x - x_c| \rightarrow m|x - x_c| - m_b|x|. \quad (6)$$

The shape symmetry of the Bessel pendulum has been used here to set the center of mass of the displaced mass m_b at

$x=0$. Buoyancy *decreases* the oscillation frequency relative to the frequency in vacuum.

The effect of dragged air is to increase the moment of inertia of the pendulum about its pivot by some amount I_d . Therefore dragged air also *decreases* the oscillation frequency relative to that in vacuum. Computation of I_d is a subtle problem in fluid dynamics, as discussed briefly in Appendix A. Bessel realized that I_d is the same for the two pivots, provided the shape of the pendulum is symmetric and the frequency and amplitude of the swing are also the same. As the shape and motion of the pendulum are identical for the two pivot locations, the motion of the air and hence the force it exerts on the pendulum must also be identical.

With both air corrections Eq. (3) becomes

$$F'(x) \equiv \frac{\omega'(x)^2}{g} = \frac{m|x-x_c| - m_b|x|}{I_0 + m(x-x_c)^2 + I_d}. \quad (7)$$

Primes are used here and below to signify quantities that include air corrections. Due to the correction terms in m_b and I_d , the function $F'(x)$ deviates slightly from $F(x)$ and all four pivot locations for a given oscillation frequency in air ω'_0 are displaced. As we now show, the distance Δx between two of the pivots nevertheless does satisfy the simple Kater condition provided the pivots are symmetrically located about the center of volume.

A Bessel pendulum must be adjusted to have equal frequencies for two such pivots, say at $x = \pm x_0$. Assume that this adjustment has been carried out, so $F'(x_0) = F'(-x_0) = (\omega'_0)^2/g \equiv F'_0$. Just as for the Kater pendulum without air corrections, set $y = x - x_c$ and solve $F'(y) = (my - m_b x_0)/(I_0 + my^2 + I_d) = F'_0$ for y , leading to a quadratic equation with roots

$$y = \pm \frac{1}{2F'_0} - \sqrt{\frac{1}{(2F'_0)^2} - \frac{I_0 + I_d + m_b x_0/F'_0}{m}}. \quad (8)$$

This is like Eq. (4) above, but includes the two air correction terms. In addition, the pivot locations appropriate for a Bessel pendulum (Δx_1 in Fig. 1) have been selected by choosing the minus sign in front of the radical in Eq. (8).

All of the complications in this equation due to buoyancy and dragged air are in the radical. Just as for the Kater pendulum without air corrections, the radical cancels when the interpivot distance is computed, giving

$$\Delta x = \Delta y = 1/F'_0 = g/(\omega'_0)^2. \quad (9)$$

This is just the Kater condition [Eq. (1)] with the air-corrected frequency ω'_0 . This proves that buoyant and dragged-air corrections vanish for a volumetrically symmetric reversible pendulum. Without this symmetry, the radical in Eq. (8) would take on different values for the two pivot locations and the necessary cancellation would not occur.

IV. CONSTRUCTION AND OPERATION OF A BESSEL PENDULUM

In this section we describe a Bessel pendulum that we have successfully used as part of a laboratory course for junior-level physics majors. The pendulum consists of two large cylindrical bobs and two small trimming collars affixed to a central rod by setscrews (Fig. 3). To achieve the necessary mass asymmetry while maintaining shape symmetry,

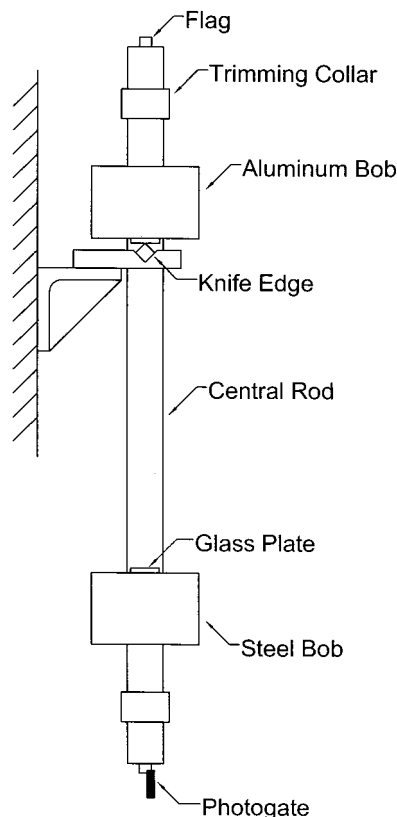


Fig. 3. Side view of the Bessel pendulum (not to scale). The pendulum swings in the plane of the figure, and can be inverted so the steel bob is uppermost. See the text and Table I for further details.

one of the bobs is aluminum and the other bob is steel. The trimming collars are aluminum, and the central rod is steel. Two sets of glass bearing plates, cut from standard microscope slides, are fastened to the bobs using cyanoacrylate cement (“superglue”). These plates are readily replaceable, which proves necessary in routine teaching-lab use. The pendulum swings on a pair of hardened steel knife edges which are mounted to a 1.3-cm-thick steel plate with a cutout for the pendulum shaft. After mounting on the plate, the knife edges were ground simultaneously to a 90° included angle. This ensures that the two knife edges are perfectly in line with one another. The plate is bolted to an aluminum bracket that is firmly fastened to a concrete column in the laboratory room. The knife edges are leveled to within 10^{-3} rad by temporarily attaching a fine thread and small weight on the side of the pendulum as a plumb bob.

Lack of rigidity of the support can be a major source of error for pendulum-based measurements of g .^{3,6} We initially mounted our knife edges so that the pendulum swung parallel to the concrete column face. With this arrangement the value of g we measured was about 250 ppm less than independent g data which are detailed below. We subsequently rotated the steel plate by 90° so the pendulum swings perpendicularly to the column face. As the column face is rough, small copper shims were inserted between the aluminum bracket and the column directly behind each knife edge. Together these changes result in short, direct mechanical connections between the knife edges and the column. With the new mounting arrangement, our measured g value is about 200 ppm larger and agrees better with the independent data. Despite the relatively massive dimensions of the steel

Table I. Dimensions of the principal parts of the pendulum.

Part	Length	Outside diameter
Central rod	121.92 cm (48 in.)	3.81 cm (1.5 in.)
Bobs	7.62 cm (3 in.)	11.43 cm (4.5 in.)
Trimming collars	3.175 cm (1.25 in.)	5.08 cm (2 in.)

mounting plate, the flexibility of the original arrangement (particularly for the knife edge further from the column) apparently caused a significant systematic error. Both the sign and approximate magnitude of this error can be understood from a simple model discussed in Appendix B.

Table I gives the dimensions for the central rod, bobs, and trimming collars. Our pendulum is perhaps larger and more massive than is necessary for successful operation. Its design resulted when the bobs and trimming collars were added to a precision physical pendulum made from the central rod alone, to convert it to a Bessel pendulum. The central rod is a standard precision machine shaft, which was chosen as an inexpensive, massive object with precise dimensions. For a Bessel pendulum, it is not necessary to know the precise dimensions of the parts and a less massive central rod could be used, allowing the bobs to be smaller. With the dimensions shown in Table I the period is approximately 1.76 s and the distance between bearing surfaces is approximately 77 cm when the pendulum is adjusted correctly.

The swinging of the pendulum is detected optically by an integrated photogate (Omron EE-SG3M), which generates a logic signal controlled by the presence or absence of an opaque object in a 4-mm-wide gap. To activate the photogate, small flags made of shim stock or cardboard are affixed to the ends of the central rod with tape or glue. The photogate is mounted to an adjustable stand on the laboratory floor, and is manually positioned near one end of the pendulum swing so it is activated only once per oscillation period. The photogate output is timed by an electronic frequency counter. We have successfully used Hewlett-Packard models 5385A and 34401A for this purpose. For the data shown below, the counter was set to display the average of 20 successive period measurements.

In general the periods of a Kater or Bessel pendulum can be trimmed by adjusting the pivot positions, the mass distribution, or both. In our design, moving the bobs changes both the pivot positions and mass distribution, while moving the collars changes only the latter. The pendulum is operated as follows. The bobs and trimming collars are always moved in pairs to maintain the overall shape symmetry of the pendulum. Define Δt as the period of the pendulum when the steel bob is down, minus the period when the aluminum bob is down. First, the bobs are positioned so that Δt changes sign when the trimming collars are moved from one extreme position (at the ends of the central rod) to the other (against the bobs). Then, leaving the bob positions fixed the two periods are carefully measured for a series of positions of the trimming collars. Curves are fit through these data to determine the period $t = 2\pi/\omega'_0$ that would be observed if the collars were adjusted so $\Delta t = 0$. Figure 4 shows data taken in this manner. Note that it is not necessary to actually adjust the collars for exact equality of the two periods.¹²

Although the dominant air corrections are canceled by the construction of the Bessel pendulum, other types of correction remain. Among these are corrections for the finite am-

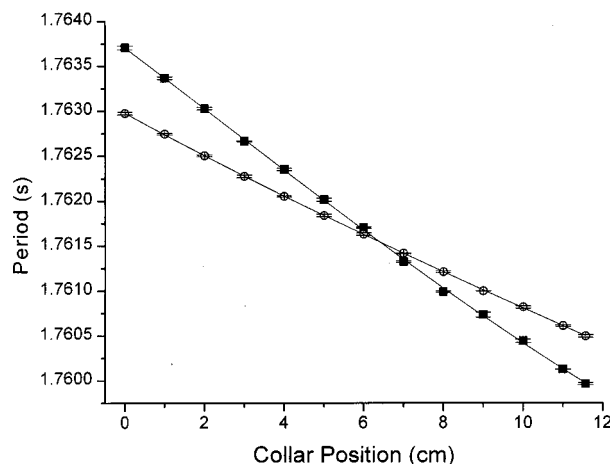


Fig. 4. Period of the pendulum measured with the aluminum bob down (closed squares) and with the steel bob down (open circles) as a function of the position of the trimming collars. The collar position was measured as the distance between the outer end of the collar and the end of the central rod. These data were taken with angular oscillation amplitude $\theta_0 = 4 \times 10^{-3}$ rad. The curves show cubic fits to the data. From the intersection of the 95% confidence bands for these two fits, the trimmed period of the pendulum is determined to be 1.761 536(54) s with 90% confidence.

plitude of swing of the pendulum, and for the damping shift of the frequency. Both corrections are thoroughly discussed in Ref. 8. For our pendulum, the damping shift is generally negligible while the finite-amplitude correction must sometimes be included.¹³ Our students are required to calculate both corrections quantitatively, and either include them or prove them to be negligible. They must also devise ways to measure the amplitude and damping. As these are small corrections, simple measurement schemes generally suffice.

A possible source of error is misplacement of the pendulum on the knife edges. By measuring the effect of purposely misplacing the pendulum by a known amount, students can quantify and control this error. A mechanical device to reproducibly and gently lower the pendulum onto the knife edges could be devised to eliminate this error. Other error sources that could be considered include bending of the knife edges and stretching and bending of the pendulum itself, as well as interactions between the pendulum and the Earth's magnetic field. Some of these are readily computed, while others are complex and poorly understood.^{6,8}

To reduce the measured period to a value for g , it is necessary to measure the distance Δx between the glass bearing plates on the pendulum as accurately as possible. This typically proves to be a significant source of uncertainty in a careful measurement of g with our pendulum, suggesting that a better measurement method for Δx than the two we have devised would be desirable. For the first method, we fabricated a metal gauge rod about 1 cm shorter than the typical trimmed distance between the bearing plates, and measured its length to within $25 \mu\text{m}$ (0.001 in.), at a specified temperature. The students use this gauge rod along with a digital caliper or a feeler gauge to measure Δx . For the second method, we used the setscrews to lock the bobs in place and then had our shop personnel measure the distance between bearing plates using their most accurate instrument, which in our case was a 76.2-cm (30 in.) inside micrometer. To maintain the precision of this measurement the temperature of the pendulum must be noted both when it is measured and when

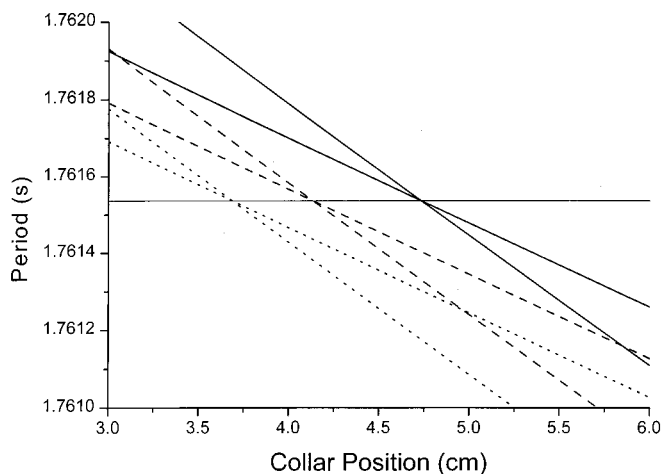


Fig. 5. Calculated periods for our pendulum with and without air corrections. The solid curves show periods calculated including both buoyancy and dragged air. The dashed curves omit buoyancy while the dotted curves omit both buoyancy and dragged air, as would occur if the pendulum were operated in vacuum. For each pair of curves, the steeper curve is for the aluminum bob down and the shallower curve is for the steel bob down. Local gravity g and the interpivot distance Δx were set equal to the values measured for our pendulum, hence the trimmed period is also the same as measured. As the horizontal line shows, the trimmed period is independent of air corrections. These curves were calculated using the nominal dimensions of the pendulum and typical densities for steel and aluminum, with no adjustable parameters. The collar position at which the periods are equal could be adjusted to agree with the data (Fig. 4) by adjusting the material densities by about 1%, well within our uncertainty.

it is used, and the change in length due to thermal expansion must be calculated. The second method achieves somewhat greater accuracy, but does not allow the students to explore the effects of moving the bobs on the central shaft.

To determine whether the experiment actually measures the local value of g with the expected accuracy, it is important to have a reliable independent value. The customary unit for tabulations of g is Gal = cm/s². An internet-accessible database of absolute values of g at many reference stations on the surface of the Earth is maintained by the Bureau Gravimétrique International (BGI).¹⁴ Alternatively, the “International Gravity Formula 1980” may be used to approximate g at mean sea level as a function of latitude ϕ .¹⁵ Omitting terms smaller than 1 mGal, this formula reads

$$g = (978.0327 \text{ Gal})(1 + 5.2790414 \times 10^{-3} \sin^2 \phi + 2.32718 \times 10^{-5} \sin^4 \phi). \quad (10)$$

Deviations from the formula due to local density variations are typically on the order of tens of mGal, while temporal variations of g at a position fixed on the Earth (due mostly to tides) are about 0.3 mGal.¹⁵ In all cases a correction must be applied for the difference in height between the pendulum and the independent g datum.¹⁶

Using the period data shown in Fig. 4 along with a measured interpivot distance $\Delta x = 77.05100(76)$ cm, we find $g = 980.291(62)$ Gal at the location of our Bessel pendulum (latitude 42.3914°, longitude -72.5258°, ground height 70 m above sea level plus additional free-air height 5 m). Our stated uncertainties are 90% confidence intervals (approximately $\pm 2\sigma$). At the BGI reference station nearest to our pendulum (3.95 km distant and 24 m lower in height) the tabulated $g = 980.36345(20)$ Gal. Corrected to the height

and latitude of our pendulum this gives $g = 980.361$ Gal, while the International Gravity Formula gives $g = 980.369$ Gal. Thus our measurement is 68 ppm smaller than the value inferred from BGI data, which may be compared with our stated uncertainty of 63 ppm.

How big are the atmospheric effects for which Bessel’s pendulum corrects? To address this question we have used the equation for the frequency of a physical pendulum, Eq. (2), to directly compute the expected periods for our pendulum both with and without buoyancy and dragged-air corrections (Fig. 5). For these calculations, the positions of the bobs and pivots were assumed to be fixed and only the collar positions were varied. As can be seen from the vertical separation of the various curves in Fig. 5, the shifts in period due to buoyancy and dragged air are a few parts in 10^{-4} . This could be anticipated from the relative densities of air and steel. It also can be seen that both buoyancy and dragged air increase the period at fixed collar position, and that the two corrections are similar in magnitude.

The period at which the curves intersect is independent of which air corrections are included in the calculation (horizontal line in Fig. 5). Thus, the measured value of g is the same for a Bessel pendulum swinging in air or swinging in vacuum. This would not be true for an asymmetrically shaped pendulum, and graphically demonstrates that Bessel’s improvement to the Kater pendulum really works.

ACKNOWLEDGMENT

This work was supported by the NSF Instrumentation and Laboratory Improvement program under Grant No. DUE-9751231.

APPENDIX A: INERTIA DUE TO DRAGGED AIR

For measurements of g with a Bessel pendulum, the moment of inertia I_d added by dragged air need not be known, as it cancels in going from Eq. (8) to Eq. (9). Nevertheless, it may be interesting to know the origin and approximate value of I_d . The existence of an effective added mass due to motion of the air was noted by Du Buat in 1786, and independently by Bessel in 1828.⁸ Analytical expressions for the inertial and damping forces on oscillating bodies immersed in viscous fluids were derived by Stokes in 1851.¹⁷ For a more detailed discussion of the dragged air mass than is given here, see Ref. 8.

When a solid body undergoes oscillatory motion in a viscous fluid such as air, the flow is rotational in a layer of characteristic thickness δ and irrotational outside this layer. The distance δ is called the viscous penetration depth, given by

$$\delta = (2\nu/\omega)^{1/2}, \quad (A1)$$

where ω is the angular oscillation frequency and ν is the kinematic viscosity ($\nu = 0.15$ cm²/s for air in standard conditions).¹⁸ When δ is much less than the dimensions of the oscillating body, fluid motion outside the thin rotational layer is the same as for an inviscid liquid and the added mass can be computed from the corresponding inviscid flow problem. For example, the added mass is one-half the mass of the displaced fluid for a spherical body, and equal to the mass of the displaced fluid for an infinitely long cylindrical body.¹⁸ Although there is no simple expression for a body of arbitrary shape, it can be seen that the total added mass m_d due

to dragged air is comparable to the displaced air mass m_b for small penetration depth δ .

If δ is made similar to or larger than the dimensions of the body (for example, by reducing the frequency of oscillation), the rotational layer extends further into the fluid and the added mass increases. With the effect of air on pendulums in mind, Stokes derived the force on an infinitely long oscillating cylinder for any value of δ relative to the cylinder radius—his solution is expressed in terms of Bessel functions!¹⁷ Stokes' solution is only valid for small oscillation amplitude (much less than the cylinder radius, in the small- δ limit). For larger oscillation amplitude, the nonlinear term in the Navier–Stokes equation becomes important and the force due to dragged air is more difficult to calculate.^{8,18}

We may picture the dragged air as extra mass m_d distributed along the length of the pendulum. The mass distribution depends upon oscillation frequency through δ , but it is independent of oscillation amplitude for sufficiently small amplitudes. Therefore, the mass distribution for a Bessel pendulum is symmetric about the center of volume $x=0$. The parallel axis theorem can be used to express the added moment of inertia about the pivot,

$$I_d = I_{d0} + m_d x^2, \quad (\text{A2})$$

where I_{d0} is the moment of inertia of the added mass distribution about $x=0$. The pendulum described in this paper has a period of 1.8 s, giving $\delta=3$ mm. Thus, it is in the small- δ limit and $m_d \approx m_b$. For a more quantitative estimate of m_d and I_{d0} , this pendulum could be roughly modeled as a long cylinder (the central rod) plus two spheres (the bobs). This approximation was used for the calculations shown in Fig. 5.

APPENDIX B: ROUNDING OF THE KNIFE EDGES AND FLEXING OF THE SUPPORT

The knife edges used to support the pendulum cannot be perfectly sharp, and it is natural to suppose that this will introduce an error in the determination of g with a Kater or Bessel pendulum. Bessel showed that rounding of the knife edges has no effect to first order on the measured value of g , provided that the knife-edge radius is unchanged when the pendulum is inverted.⁴ This is automatically the case when the knife edges are stationary and the flat bearing plates are on the pendulum, as in our design. In this Appendix we outline a proof, leaving a few details for the reader to work out. We also discuss the effect on the measured value of g of flexing in the knife-edge support.

Assume that the contact area of the knife edge is cylindrical with radius r , and that the bearing plate rolls on the knife edge without slipping (both assumptions could be questioned for an actual pendulum). When the pendulum swings through an angle θ , the line on the bearing plate that contacted the knife edge at $\theta=0$ rises by an amount Δh and moves to the side by an amount Δs (Fig. 6). Elementary trigonometry shows

$$\begin{aligned} \Delta h/r &= \cos \theta + \theta \sin \theta - 1 = \theta^2/2 + O(\theta^4), \\ \Delta s/r &= \sin \theta - \theta \cos \theta = O(\theta^3). \end{aligned} \quad (\text{B1})$$

These vertical and horizontal movements of the pendulum are in addition to the ordinary rotational movement. The simplest way to deduce their effect on the oscillation frequency is to consider the pendulum's kinetic and potential energy.¹⁹ For small oscillations the kinetic energy of the pendulum is

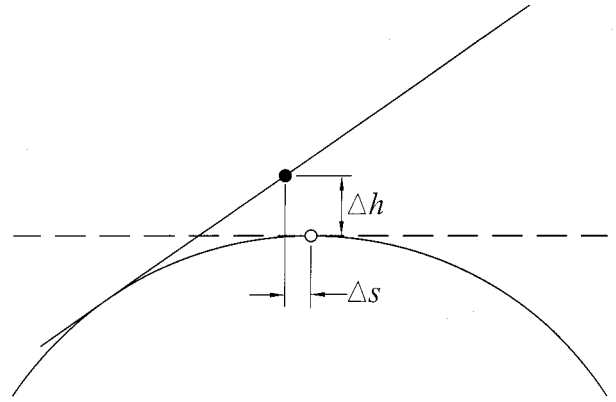


Fig. 6. Diagram used to compute the rise Δh and horizontal shift Δs of the pendulum due to the finite radius of the knife edge. The circular arc represents the knife edge. The dashed line represents the bearing plate when the pendulum is vertical, while the solid line represents the bearing plate when the pendulum is at an angle $\theta \neq 0$. When the pendulum swings away from vertical, the line on the bearing plate that is initially in contact with the knife edge moves from the position of the open circle to the position of the closed circle, assuming rolling contact between the knife edge and bearing plate.

due to horizontal velocities of the various parts. For perfectly sharp knife edges, these velocities are proportional to $\dot{\theta}$. The additional horizontal velocity due to knife-edge rounding is $\Delta s \sim \theta^2 \dot{\theta}$, and so has no effect on the frequency for $\theta \rightarrow 0$.

The vertical movement Δh is of the same order in θ as the rise in the center of mass for a zero-radius knife edge, $l\theta^2/2$. Therefore Δh changes the potential energy as if the distance between the pivot and the center of mass were increased by r . This adds a term mr to the numerator of Eq. (3) or (7). The added term is the same for both positions of the pendulum, so it cancels when the interpivot distance is computed, just like the buoyancy correction.

Another potential source of error associated with the knife-edge pivots is flexibility that allows them to move as the pendulum swings. Unfortunately, flexibility in the knife-edge support results in horizontal motion of order θ , and so gives a first-order error in the g measurement. The only horizontal force on the pendulum is transmitted through the pivots. We model the support as a horizontal spring with spring constant k . Computing the force exerted by this spring as the mass m of the pendulum times the horizontal acceleration of the center of mass, the horizontal motion of the pivot is

$$\Delta s = (m\omega^2/k)l\theta \equiv \epsilon l\theta, \quad (\text{B2})$$

where l is the distance between pivot and center of mass.²⁰ As the movement of the pivot should be much smaller than the movement of the pendulum center of mass, we can assume $\epsilon \ll 1$.

The total kinetic energy of the pendulum is the sum of energies for rotation about the center of mass and translation of the center of mass,

$$\begin{aligned} E_k &= I_0 \dot{\theta}^2/2 + m(l\dot{\theta} + \dot{\Delta s})^2/2 = [I_0 + ml(1 + \epsilon)^2] \dot{\theta}^2/2 \\ &\approx [I_0 + ml^2(1 + 2\epsilon)] \dot{\theta}^2/2. \end{aligned} \quad (\text{B3})$$

Therefore, the term in m in the denominators of Eqs. (3) and (7) is modified as

$$m(x - x_c)^2 \rightarrow m(1 + 2\epsilon)(x - x_c)^2. \quad (\text{B4})$$

With this substitution it is easily verified that the Kater condition, Eq. (1), is changed to

$$\omega_0^2 = g/[\Delta x(1 + 2\epsilon)]. \quad (\text{B5})$$

Thus, the apparent value of g is fractionally less than the true value of g by $2\epsilon = 2m\omega^2/k$. Our pendulum has $m = 18.5 \text{ kg}$, $\omega = 2\pi/(1.76 \text{ s})$. To achieve an error due to support flex $2\epsilon \leq 10^{-5}$, we require $k \geq 4.7 \times 10^7 \text{ N/m}$. We may imagine a support consisting of horizontal rods of length L and total cross-sectional area A connecting the pendulum pivots to an infinitely massive wall. If the Young's modulus of the support rods is E , their effective spring constant is $k = AE/L$. If we use aluminum support rods 10 cm long for our pendulum ($E = 7 \times 10^{10} \text{ N/m}^2$), their total cross-sectional area must be at least 0.7 cm^2 to achieve $2\epsilon \leq 10^{-5}$. For less favorable geometries, like our initial arrangement with the pendulum swinging parallel to the wall, correspondingly more massive support is required.

It is also interesting to calculate the actual support flex under operating conditions, using Eq. (B2). For our pendulum the mean $l = 39 \text{ cm}$ and we typically use swing amplitude $\theta_0 \approx 4 \times 10^{-3} \text{ rad}$. Therefore, if the pivot support is stiff enough to give $2\epsilon \leq 10^{-5}$, the amplitude Δs_0 of the pivot movement must be no more than 8 nm. This is about one-seventieth of a wavelength of visible light. In the era of precision pendulum measurements of gravity, optical interferometers were used to measure this small pivot movement and sometimes two matched pendulums were swung out of phase from the same support in an effort to minimize it.³

^aElectronic mail: candela@physics.umass.edu

^bPresent address: Physics Department, Amherst College, Amherst, MA 01002.

¹D. Kleppner and R. J. Kolenkow, *An Introduction to Mechanics* (McGraw-Hill, New York, 1973), pp. 257–258.

²J. B. Marion, *Classical Dynamics of Particles and Systems* (Sanders College Publishing, Fort Worth, 1995), 4th ed., p. 455.

³V. F. Lenzen and R. P. Multhaupt, *Development of Gravity Pendulums in the 19th Century*, Contributions from the Museum of History and Technology Paper 44 (Smithsonian Institution, Washington, 1965), pp. 303–352.

⁴F. W. Bessel, “Untersuchungen über die Länge des einfachen Secundenpendels,” *Abhandlungen der Königl. Akademie der Wissenschaften zu Berlin* (1826); also published as *Untersuchungen über die Länge des einfachen Secundenpendels* (Bruns, Leipzig, 1889).

⁵Precision pendulums based on Bessel's design were first constructed in 1861 (after Bessel's death) by the firm A. Repsold and Sons, hence the

Bessel pendulum is often called the Repsold–Bessel or Bessel–Repsold reversible pendulum.

⁶A. H. Cook, “The Absolute Determination of the Acceleration Due to Gravity,” *Metrologia* **1**, 84–114 (1965).

⁷I. Marson and J. E. Faller, “ g —the acceleration of gravity: Its measurement and its importance,” *J. Phys. E* **19**, 22–32 (1986).

⁸R. A. Nelson and M. G. Olsson, “The pendulum—Rich physics from a simple system,” *Am. J. Phys.* **54**, 112–121 (1986).

⁹R. D. Peters, “Student-Friendly Precision Pendulum,” *Phys. Teach.* **37**, 390–393 (1999).

¹⁰A. Dupré and P. Janssen, “An accurate determination of the acceleration of gravity g in the undergraduate laboratory,” *Am. J. Phys.* **68**, 704–711 (2000).

¹¹The frequency shift due to viscous *damping* by the air remains present in a Bessel pendulum, and must be corrected for if significant.

¹²K. E. Jesse, “Kater pendulum modification,” *Am. J. Phys.* **48**, 785–786 (1980).

¹³The finite-amplitude correction is the same for a physical pendulum as it is for a simple pendulum. As the fractional change in period is simply a function of the angular oscillation amplitude θ_0 , the Kater and Bessel pendulums can be adjusted for reversibility at fixed, finite θ_0 . Then the finite-amplitude correction for this θ_0 is applied before using the Kater relation to determine g .

¹⁴Internet address: bgi.cnes.fr

¹⁵P. Vaníček and E. Krakiwsky, *Geodesy: The Concepts* (North-Holland, Amsterdam, 1986), 2nd ed., p. 79.

¹⁶The height correction for locally flat topography is $\Delta g/\Delta h = [-2 + (3/2) \times (\rho_c/\rho_e)]g/R_e$ where Δh is the height difference and ρ_e and R_e are the mean density and radius of the Earth, respectively. The mean density of the local crust material beneath the higher of the two points being compared is ρ_c . The first term expresses the $1/R^2$ dependence of gravity in free space, while the second accounts for the gravitational attraction of the local material. The second term (the so-called Bouguer correction) is comparable in size to the first and cannot be omitted. For example, the free-air ($\rho_c = 0$) gravity gradient is $\Delta g/\Delta h = -3.08 \text{ mGal/m}$ while for typical $\rho_c/\rho_e \approx 0.5$ we have $\Delta g/\Delta h \approx -2 \text{ mGal/m}$. The second term is easily derived by modeling the local material as a disk much wider than it is thick, but much smaller than the Earth. For a more detailed discussion including the effects of topography, see Ref. 15, Chap. 21.

¹⁷G. G. Stokes, *Trans. Cambridge Philos. Soc. (II)* **9**, 8 (1851); *Mathematical and Physical Papers* (Cambridge U.P., London, 1922), Vol. 3, p. 1 (1901).

¹⁸L. D. Landau and E. M. Lifshitz, *Fluid Mechanics* (Pergamon, Oxford, 1987), 2nd ed., p. 83ff.

¹⁹The pendulum is a simple harmonic oscillator with potential energy $E_p = A\theta^2/2$ and kinetic energy $E_k = B\dot{\theta}^2/2$. Using energy conservation $\dot{E}_p = -\dot{E}_k$ gives $\ddot{\theta} = -(A/B)\theta$, hence $\omega^2 = A/B$. For the pendulum A is g times the numerator of Eq. (3) or (7), while B is the denominator.

²⁰In writing Eq. (B2) we assume that the resonant frequency of the support for horizontal vibrations is much greater than the frequency of the pendulum. In this limit the mass of the support can be ignored.